ELSEVIER

Polymer 42 (2001) 4347–4352

polymer

www.elsevier.nl/locate/polymer

Super-selective polysulfone hollow fiber membranes for gas separation: rheological assessment of the spinning solution

S.A. Gordeyev[a], G.B. Lees[a], I.R. Dunkin[b], S.J. Shilton[a,*]

[a]*Department of Chemical and Process Engineering, University of Strathclyde, James Weir Building, 75 Montrose Street, Glasgow G1 1XJ, Scotland, UK*
[b]*Department of Pure and Applied Chemistry, University of Strathclyde, Thomas Graham Building, 295 Cathedral Street, Glasgow G1 1XL, Scotland, UK*

Received 15 June 2000; received in revised form 16 October 2000; accepted 20 October 2000

Abstract

A polysulfone spinning solution used recently to produce enhanced selectivity gas separation hollow fiber membranes was rheologically assessed using a rotational rheometer and an optical shear cell. Effects of temperature and shear rate on viscosity, power law behavior and normal force provided some clues regarding phase inversion and molecular orientation. At relatively low temperatures, phase inversion may occur in the absence of a shear field. At moderately low temperatures, phase inversion may be induced by applied shear. At higher temperatures, phase inversion is not induced by shear but rather shear induces molecular orientation.

The results suggest that, unless spinning at low temperature, extrusion shear does not directly induce demixing during membrane formation but, instead, is linked indirectly to phase inversion through induced molecular orientation which, in turn, affects the subsequent dry or wet precipitation stages in spinning. This work is a step towards the construction of phase diagrams and determining their distortion in shear fields. Such knowledge, coupled with deeper insights into induced polymer molecule orientation, would enable further improvements in spinning techniques and membrane performance.

Keywords: Rheology; Hollow fiber spinning; Phase inversion

1. Introduction

Hollow fiber gas separation membranes are produced by spinning a polymer solution. Controlled phase separation of this solution, or dope, via dry and immersion precipitation to form a thin and undamaged membrane active layer is the cornerstone of the process. Recently, using a particular forced convection dry/wet spinning approach, polysulfone membranes with elevated values of selectivity were produced [1,2]. A multi-component dope (comprising polymer, two good solvents, one of which is highly volatile, and a non-solvent) was extruded through an annulus in which it was subjected to shear flow. The hollow filament was then passed through a dry forced convection chamber where the volatile solvent was driven off producing the membrane outer skin (active layer). Spinodal precipitation and coalescence of the polymer rich phase through capillary pressure were the likely mechanisms of skin formation [3]. The near-cloud-point composition of the dope (used by Pesek and Koros to cast flat sheet membranes [4]) and the aggressiveness of the specific forced convection conditions employed, resulted in effectively instantaneous skin formation. Therefore, a level of shear induced polymer molecular orientation was locked into the membrane active layer before relaxation could occur. This enhanced orientation has been measured using spectroscopy [5,6] and investigated through free volume measurements [1]. It is thought that molecular orientation alters the molecular conformation and hence gas transmission properties of the membrane skin resulting in elevated selectivities. Effects of shear induced molecular orientation in the spin line on fiber performance have now also been observed by Chung et al for both gas separation [7] and ultrafiltration membranes [8].

A bore fluid is also necessary in the production of hollow fibers and this is injected into the emerging hollow filament through the center of the extrusion annulus of the spinneret. The encroachment of the inner coagulation front upon the outer skin layer should be retarded in order to preserve the delicate outer active layer structure [9]. This was achieved by using a bore fluid of reduced non-solvent (water) activity to slow down phase inversion from within. Membrane spinning is completed by passing the spin line through an

* Corresponding author. Tel.: +44-141-552-4400, ext. 2380; fax: +44-141-552-2302.
E-mail address: simon.shilton@strath.ac.uk (S.J. Shilton).

0032-3861/01/$ - see front matter
PII: S0032-3861(00)00787-4

Nomenclature

d	Gap height (m)
F_c	Centrifugal force (N)
K	Power law constant (Pa s^n)
n	Power law index (–)
r	Radius (m)
Greek symbols	
$\dot{\gamma}$	Shear rate (s^{-1})
η	Viscosity (Pa s)
τ	Shear stress (Pa)
ω	Angular velocity (rad s^{-1})

external non-solvent (usually water) coagulation bath and then collecting the fiber on a wind-up drum.

It is known that shear fields influence the demixing dynamics of polymer systems [10,11]. Thus, as well as having an influence on molecular alignment, extrusion shear, experienced by the dope, is likely to affect the polymer precipitation mechanism during membrane formation. In fact, effects of shear during hollow fiber spinning on membrane skin production and substructure morphology have been investigated recently [9].

Most of the published studies of membrane forming polymer solutions focus on the influence of temperature and composition on membrane properties. Only a few report the rheology of spinning solutions [12,13]. In the recent past, the polysulfone spinning solution employed in our laboratory to spin super-selective hollow fiber membranes was briefly tested rheologically to find power law parameters [1]. These were then used to estimate the shear rate profile in the spinneret during hollow fiber production [14]. However, given the importance of rheological factors in membrane production, a more detailed investigation of that spinning solution was felt necessary. That investigation is the subject of this report.

2. Experimental

2.1. Polymer solution (dope) preparation

The four component dope (22 wt.% polysulfone, 31.8 wt.% *N*,*N*-dimethylacetamide, 31.8 wt.% tetrahydrofuran (THF) and 14.4 wt.% ethanol) that was used previously to produce enhanced selectivity hollow fiber membranes [1,2] was studied in this work. Polysulfone (Amoco Chemicals, Udel P1700, weight-average molecular weight 35 400) was dissolved in the blend of solvents by intensive mixing at 80°C. Next, the solution was cooled down to 50°C and the ethanol (non-solvent) was added keeping the solution intensively mixed to dissolve white flakes of local precipitation. Finally, the dope was kept at 50°C until fully degassed and then cooled down slowly to ambient temperature. The dope was stored in a glass bottle at 25°C.

2.2. Rheometer

The steady state flow properties of the dope were measured using a TA Instruments AR 1000 Rotational Rheometer. Because of high dope sensitivity to environmental conditions and loading procedure, some preliminary studies were conducted to establish the test parameters that provided a high level of reliability in a wide range of protocols. Reliable and consistent results were achieved using a 2 cm parallel plate geometry with a test duration of 5 min. The standard gap size for the tests was 100 μm and a 20 s period of pre-shear at a minimum shear rate was employed at the start of each test.

In addition, it was necessary to shroud the geometry with a solvent trap to hinder evaporation of THF, a highly volatile solvent, from the sample rim. The local environment was equilibrated with the sample by depositing a ring of dope within the solvent trap. Under these conditions, there was found to be no effect on flow behavior of using a continuous ramped experiment in comparison to a stepped one and the former regime was used throughout this study. Each flow curve was obtained as an average of at least five measurements.

2.3. Optical shear cell

An optical shear cell was built for this study to observe visually the dope behavior under shear. The sample was located between two parallel glass discs of diameter 40 mm. The upper disc was fixed and the bottom one was attached to a driving gear that was rotated by a variable speed motor. The gap between the discs was determined by precision spacers placed between the upper and lower stainless steel housings. The sample was illuminated by scattered white light from below and observed from above.

For parallel plate measurements, the shear rate $\dot{\gamma}$ is a linear function of the sample radius given by

$$\dot{\gamma} = \omega r/d$$

The shear rate is at a maximum at the outer edge of the sample and decreases to zero in the center. Three gaps of 250, 500 and 750 μm and a maximum rotational speed of about 105 rad s^{-1} were used in this study providing a maximum shear rate achievable of about 8400 s^{-1}. These conditions accurately reflect those experienced in the rheometer.

3. Results and discussion

3.1. Flow curve at 25°C

The viscosity and normal force exerted by the dope as functions of shear rate measured at 25°C are shown in Fig. 1. Four distinct regions (I–IV) of behavior can be detected. At very low shear rates (region I, below 1 s^{-1}) fluctuations and non-linear behavior of viscosity were observed probably

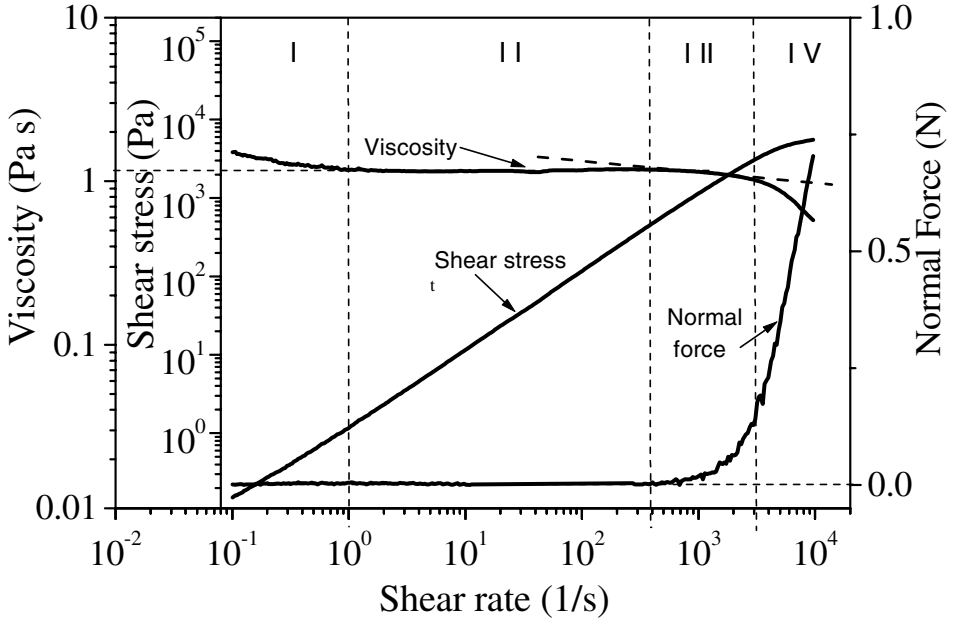

Fig. 1. Flow curve with normal force at 25°C.

due to limitations in instrument precision. However, it can be seen that in a wide range of shear rates (region II) the dope behaves as a Newtonian liquid with a viscosity of 1.2 Pa s. No normal force is detected in this region. However, a normal force begins to be exerted after a certain shear rate, designated as the first critical shear rate (FCSR). This indicates the beginning of deviation from Newtonian behavior and coincides with a decrease in viscosity with increasing shear rate (region III). The flow curve in this region is fitted well by a power law $\eta = K\dot{\gamma}^{n-1}$, where $n = 0.925$ and $K = 2.06$ Pa s^n.

At an even higher shear rate there exists a further gradient change termed the second critical shear rate (SCSR) beyond which viscosity decreases more rapidly with increasing shear rate (region IV). This effect is often observed with rotational rheometers at high rotational speed and is associated with sample loss induced by high centrifugal forces.

3.2. Optical shear cell

Room temperature tests were performed at various rotational speeds and gap settings. (At each gap setting, the speed was increased in steps.) During these experiments, fragments of the fluid sample were thrown out of the apparatus resulting in a decrease in sample diameter. It was found that a constant sample diameter was obtained after 30–40 s at each speed. This sample loss was attributed to centrifugal force where

$$F_c \propto \omega^2 r$$

The radius of the sample remaining in the cell after each

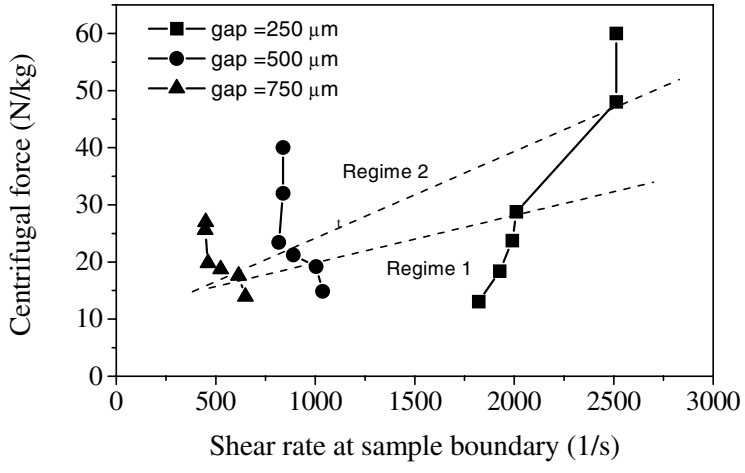

Fig. 2. Optical shear cell data.

speed was measured. Using this radius, the centrifugal force that the dope could withstand and the shear rate experienced were determined. The results of the observations are given in Fig. 2 where centrifugal force (which is representative of fluid strength under elongation) is plotted against the corresponding shear rate for each gap setting.

Although data interpretation is difficult, the dope seems to experience different strength (and possibly micro-structural) regimes. An upper and lower regime have been identified at each gap setting and are shown in Fig. 2. For both regimes the fluid is able to withstand greater centrifugal force at higher shear rates as gap decreases: for a 750 μm gap, the first strength regime (regime 1) forms at around 600 s^{-1} and can withstand centrifugal forces of up to 18 N kg^{-1} whereas for a 250 μm gap, the structure forms at about 2000 s^{-1} and can withstand centrifugal forces of up to 28 N kg^{-1}. A similar picture can be painted for the second or upper regime. Also, the resistance of the dope to centrifugal forces is greater in the second regime than in the first.

Generally, it can be seen that as gap decreases, the resistance of the dope to centrifugal force increases and this resistance occurs at higher shear rates. No meaningful visible changes in sample transparency were noticed throughout the shear cell tests.

3.3. Rheometer: varying gaps to investigate centrifugal force

To investigate the assumption that the SCSR was mainly due to the onset of sample loss due to centrifugal force, flow curves were obtained for a range of gap settings (50, 200 and 500 μm) using a 2 cm parallel plate geometry at 25°C. In this way, shear rate and centrifugal force could be studied separately. The results are shown in Table 1 where the first and second critical shear rates are given with the corresponding centrifugal forces.

The data in Table 1 show that the onset of the first non-Newtonian region (FCSR) is shear rate dependent occurring at around 400 s^{-1} at 25°C. This confirms that the initial onset of shear thinning in the dope is a true rheological phenomenon as supported by the appearance of normal force. The onset of the second region of non-linear behavior occurs at a particular centrifugal force (SCCF) of about 16 N kg^{-1} regardless of the shear rate. This suggests that the second non-linear region in the flow curve is caused by centrifugal sample loss which starts at about 16 N kg^{-1}.

Table 1
Effect of gap on onset of shear thinning and sample loss regimes (25°C)

Gap (μm)	FCSR (s^{-1})	Centrifugal force at FCSR (N kg^{-1})	SCSR (s^{-1})	Centrifugal force at SCSR (N kg^{-1})
50	411	0.04	7720	14.9
200	370	0.54	2020	16.3
500	374	3.50	795	15.8

At 25°C the power law parameters during the region of true non-Newtonian behavior were found to be $n = 0.925$ and $K = 2.06$ Pa s^n. This shows that the non-linearity is in fact weaker than quoted previously for the dope at the slightly different temperature of 20°C ($n = 0.693$, $K = 43.1$ Pa s^n) [1]. This is not surprising as the previous results would have been affected by the sample loss discovered here and, in addition, the previous tests did not involve a solvent trap.

The conclusions regarding a threshold centrifugal force of about 16 N kg^{-1} for sample loss are supported by the optical shear cell tests. Fig. 2 shows that sample loss starts at a similar centrifugal force of about 15 N kg^{-1} for all gap settings.

Further evidence that sample loss is in fact occurring rather than an alternative phenomenon like shear fracturing [15] is that the flow behavior of the dope above SCSR is not recoverable.

3.4. Rheometer: effects of temperature and shear

A number of flow curves were established over the

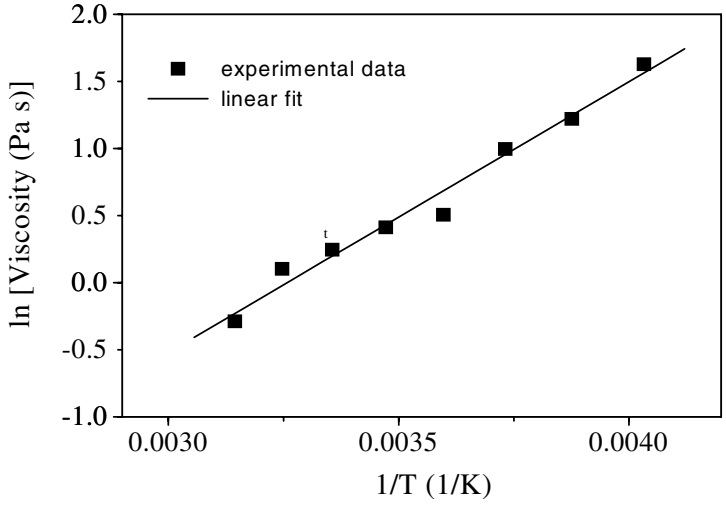

Fig. 3. Arrhenius plot for the viscosity of the spinning solution.

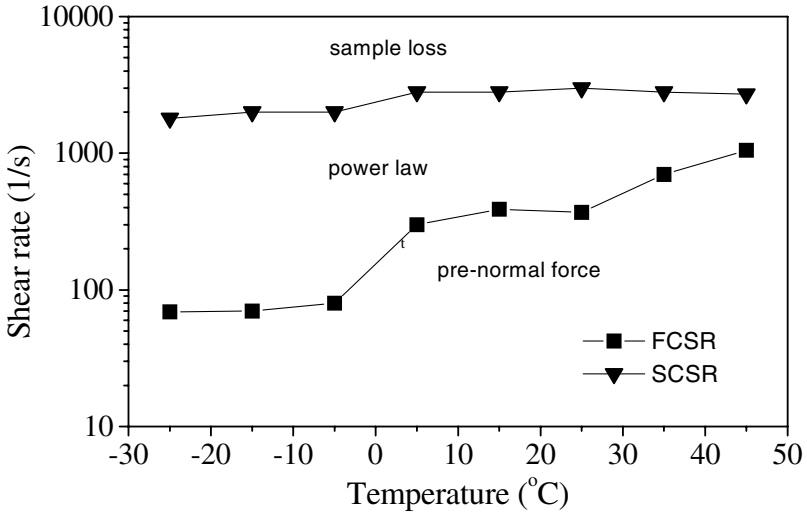

Fig. 4. Effect of temperature on FCSR and SCSR.

temperature range −25°C to +45°C. At each temperature, values were measured for the FCSR and SCSR, for the viscosity at the FCSR, the normal force at the SCSR, and for the power law index and constant for the power law region. The viscosity was found to decrease with increasing temperature according to an Arrhenius relationship as shown in Fig. 3.

Fig. 4 shows the FCSR and SCSR plotted against temperature. The plots demarcate the regions of different rheological behavior (pre-normal force, power law and sample loss). The commencement of sample loss (SCSR) is less sensitive to temperature than the onset of power law behavior (FCSR). The other parameters; power law index and constant for power law region, and normal force at SCSR are shown in Table 2.

Given the data in Fig. 4 and Table 2, there would appear to be an interesting transition at around −5°C as temperature decreases. The power law region begins at lower shear rates (at about 70 s^{-1} as opposed to about 400–1000 s^{-1}), larger normal forces are exerted in the power law region and the power law index switches from a $n < 1$ (thinning) to $n > 1$ (thickening). These results may provide some clues about the effect of temperature and shear rate on phase inversion.

At lower temperatures phase stability would be expected to decrease. Thus, the earlier onset of power law behavior and the shear thickening behavior ($n > 1$) at lower temperatures may be evidence of shear induced demixing of the polymer solution. In fact, a threshold shear rate of 70 s^{-1} may be required to cause phase inversion at temperatures of less than −5°C. The sizeable normal forces exerted at low temperatures may be a signature of this shear induced phase inversion.

Table 2
Effect of temperature on power law parameters and normal force

Temperature (°C)	K (Pa s^n)	n	Normal force at SCSR (N)
−25	3.72	1.063	1.85
−15	2.32	1.076	1.14
−05	2.56	1.011	0.60
+05	2.43	0.944	0.15
+15	2.28	0.935	0.19
+25	2.06	0.925	0.10
+35	1.69	0.939	0.06
+45	1.36	0.931	0.11

At temperatures above −5°C, no amount of shear can induce phase inversion but at values of about 400–1000 s^{-1}, the dope begins to exhibit viscoelastic shear thinning behavior ($n < 1$) indicative of shear induced molecular orientation. Normal forces are significant but less intense here.

At the lowest temperatures of −25 and −15°C the dope actually exhibited marked shear thickening behavior in the pre-normal force region which may indicate that the dope is cold enough to phase invert without any applied shear field.

4. Conclusions

The rheological tests carried out here have provided some clues regarding the effects of shear fields and temperature on the phase inversion of a favored membrane spinning solution. At relatively low temperatures (below −15°C) phase inversion may occur in the absence of an appreciable shear field. At moderately low temperatures (below −5°C) phase inversion may be induced at shear rates of about 70 s^{-1}. At higher temperatures (above −5°C) it would seem that phase inversion is not induced by shear but rather shear induces molecular orientation at say 400–1000 s^{-1}. This orientation is responsible for increased membrane selectivity [1,2].

The results suggest that for this particular dope, unless spinning at low temperature, shear does not directly induce demixing during membrane formation. This implies that the previously observed effects of shear on membrane morphology [9] are linked indirectly to phase inversion through induced molecular orientation which, in turn, affects the subsequent dry or wet precipitation stages in spinning.

In order to create a clearer multi-dimensional picture of the influence of shear and temperature on phase inversion during hollow fiber membrane production, a range of different dope concentrations needs to be tested. It would also be advantageous to extend the shear rate range under investigation. A capillary rheometer would allow this as sample loss would not be limiting. The optical shear cell also needs to be upgraded to allow temperature control, quantitative light scattering turbidity measurements and molecular orientation measurements through birefringence and optical dichroism.

Ultimately, the construction of phase diagrams showing their distortion under shear is intended. This knowledge coupled with further insights into induced polymer molecule orientation would help in the optimization of spinning conditions to further improve membrane performance.

Acknowledgements

The authors wish to acknowledge the financial support provided by The Engineering and Physical Sciences Research Council (UK) (Grant GR/M74955) and Air Products and Chemicals Inc. (USA). Mr J. Murphy and Mr L. Allan (Department of Chemical and Process Engineering, University of Strathclyde) are also acknowledged for the construction of the optical shear cell.

References

[1] Ismail AF, Dunkin IR, Gallivan SL, Shilton SJ. Production of super selective polysulfone hollow fiber membranes for gas separation. Polymer 1999;40(23):6499.

[2] Ismail AF, Shilton SJ. Polysulfone gas separation hollow fiber membranes with enhanced selectivity. J Mem Sci 1998;139:285.

[3] Pinnau I, Koros WJ. A qualitative skin layer formation mechanism for membranes made by dry/wet phase inversion. J Polym Sci: Part B Polym Phys 1993;31:419.

[4] Pesek SC, Koros WJ. Aqueous quenched asymmetric polysulfone membranes prepared by dry/wet phase separation. J Mem Sci 1993;81:71.

[5] Ismail AF, Shilton SJ, Dunkin IR, Gallivan SL. Direct measurement of rheologically induced molecular orientation in gas separation hollow fiber membranes and effects on selectivity. J Mem Sci 1997;126:133.

[6] Shilton SJ, Ismail AF, Gough PJ, Dunkin IR, Gallivan SL. Molecular orientation and the performance of synthetic polymeric membranes for gas separation. Polymer 1997;38(9):2215.

[7] Chung TS, Lin WH, Vora RH. The effect of shear rates on gas separation performance of 6FDA-durene polyimide hollow fibers. J Mem Sci 2000;167(1):55.

[8] Chung TS, Qin JJ, Gu J. Effect of shear rate within the spinneret on morphology, separation performance and mechanical properties of ultrafiltration polyethersulfone hollow fiber membranes. Chem Engng Sci 2000;55(6):1077.

[9] Sharpe ID, Ismail AF, Shilton SJ. A study of extrusion shear and forced convection residence time in the spinning of polysulfone hollow fiber membranes for gas separation. Sep Purification Technol 1999;17(2):101.

[10] Wolf BA. Thermodynamic theory of flowing polymer solutions and its application to phase separation. Macromolecules 1984;17:615.

[11] Gerard H, Higgins JS, Clarke N. Shear-induced demixing in polystyrene/poly(vinyl methyl ether) blends. 1. Early stages of shear-induced demixing. Macromolecules 1999;32(16):5411.

[12] Shilton SJ, Bell G, Ferguson J. The rheology of fiber spinning and the properties of hollow-fiber membranes for gas separation. Polymer 1994;35(24):5327.

[13] Torrestiana-Sanchez B, Ortiz-Basurto RI, Brito-De La Fuente E. Effect of nonsolvents on properties of spinning solutions and polyethersulfone hollow fiber ultrafiltration membranes. J Mem Sci 1999;152:19.

[14] Shilton SJ. Flow profile induced in spinneret during hollow fiber membrane spinning. J Appl Polym Sci 1997;65:1359.

[15] Walters K. Rheometry. London: Chapman and Hall, 1975.